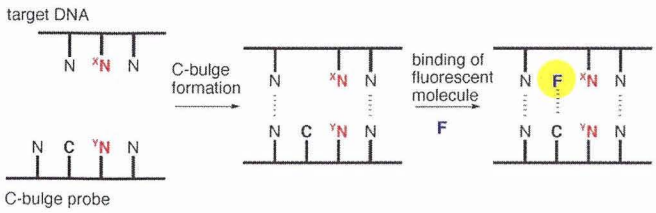

Figure 1. Illustration of the SNP typing exploiting the C-bulge binding molecule DANP and C-bulge probe as a scaffold to recruit DANP to the region directly neighbouring the SNP site. ^{X}N: nucleotide to be determined at the SNP site; ^{Y}N: nucleotide opposite ^{X}N in the probe; C: the bulged cytosine; F: fluorescent molecule binding to C-bulge (DANP).

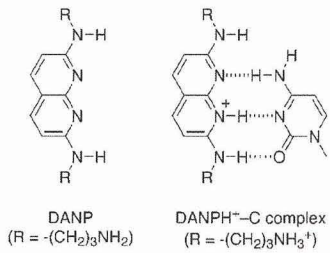

Figure 2. Structures of DANP and DANPH$^+$–C complex.

bound to the C-bulge even in the presence of unbound DANP.

The feasibility of the proposed method depends entirely on 1) the DANPH$^+$ is bound to the C-bulge flanking the mismatched base pair and 2) the DANPH$^+$ fluorescence could be modulated by the neighboring base pair. We have investigated the binding of DANP to the C-bulge flanking the mismatched base pairs and the fluorescence behavior upon binding. We report here that the fluorescence of the DANPH$^+$ bound to the C-bulge was, in fact, selectively modulated by the neighboring matched or mismatched base-pair formation. The profile in the fluorescence change of DANPH$^+$ regarding the allele specific C-bulge probes may be used for the determination of the allele type at the predetermined SNP site.

Results and Discussion

First we looked at the DANPH$^+$ binding to the C-bulge flanking the mismatched base pairs. The formation of the DANPH$^+$-bound complex was investigated by measuring the melting temperature (T_m) of the 16-mer target DNA 5′-d(ACATCCAA^{X}NCAACCAC)-3′ and 17-mer C-bulge probes 5′-d(GTGGTTG^{Y}N*C*TTGGATGT)-3′ in the presence of DANP. The C-bulge probes contained one additional cytosine (italic) flanking ^{Y}N (N = A, T, C, G, and I) opposite ^{X}N. We have used inosine (I) in addition to A, T, C, and G to avoid the fluorescence quenching by G in the C-bulge probe. Upon hybridization, a single C-bulge was produced directly neighboring the ^{X}N–^{Y}N base pair. By alternating ^{Y}N with A, T, G, C, and I with respect to four ^{X}N in the target DNA, C-bulge duplexes flanking 20 different matched and mismatched base pairs were produced. The T_m of the duplex contained ^{X}T, ^{X}A, and ^{X}C increased in the presence of DANP regardless to the base at ^{Y}N (Table 1). Based on the

Table 1. Melting temperatures of C-bulge duplexes with DANP.[a]

	5′-d(ACATCCAA_^{X}NCAACCAC)-3′ 3′-d(TGTAGGTTC^{Y}NGTTGGTG)-5′			
^{Y}N	^{X}T	^{X}A	^{X}G	^{X}C
A	52.2 (4.8)[b]	46.7 (2.7)	52.2 (0.6)	46.3 (3.9)
T	47.3 (5.3)	50.4 (3.2)	53.5 (1.0)	46.6 (5.0)
C	48.1 (5.5)	46.7 (4.0)	56.0 (2.3)	48.1 (6.7)
G	50.3 (6.0)	51.8 (2.9)	54.3 (1.1)	54.6 (3.6)
I	48.2 (5.5)	52.2 (4.2)	52.5 (0.5)	49.4 (3.1)

[a] T_m of duplexes 5′-d(ACATCCAA^{X}NCAACCAC)-3′/5′-(GTGGTTG^{Y}NCTTGGATGT)-3′ (2 μM) were measured in 10 mM Na cacodylate (pH 7.0) with 100 mM NaCl in the presence of DANP (50 μM). [b] The values in a parenthesis refer to the increase of T_m compared with the values measured without DANP. The reported values are the average of three independent measurements.

K_d value of 10 mM for the DANPH$^+$ binding to the C-bulge,[20] it was estimated that about 80% of the C-bulge duplex was present as the DANPH$^+$-bound form under these conditions. Duplexes containing ^{X}G showed much smaller increases of T_m than other duplexes especially when ^{Y}N was A, T, G, and I. This is probably due to the unavoidable formation of ^{X}G–C base pair between ^{X}G and the extra cytosine, producing a single ^{Y}N bulge instead of the C-bulge.

Having confirmed the binding of DANP to the C-bulge flanking the ^{X}T–^{Y}N, ^{X}A–^{Y}N, and ^{X}C–^{Y}N base pairs, we focused our attention on the fluorescence of the DANPH$^+$ bound to the C-bulge. The fluorescence measurements were performed in the presence of an excess amount of C-bulge duplex to make sure that DANP was completely bound to the C-bulge. The DANPH$^+$ fluorescence was selectively modulated by the base pairs flanking the C-bulge (Figure 3). Strong fluorescence was observed when the base pair flanking the C-bulge was ^{X}A–^{Y}T, whereas only weak fluorescence was observed for ^{X}C–^{Y}G. It is often observed that the guanine base quenches the fluorescence of the neighboring fluorophore.[17,21,22] We found that the substitution of G in the ^{X}C–^{Y}G base pair to I in the ^{X}C–^{Y}I base pair resulted in a large increase in the fluorescence intensity. The use of I in the C-bulge probe would be effective for suppressing the quenching of the DANPH$^+$ fluorescence by the neighboring G in the C-bulge probe. The effect of the flanking mismatched base pair on the DANPH$^+$ fluorescence was quite marked. While the DANPH$^+$ fluorescence was quite weak when the base pair flanking the C-bulge was ^{X}C–^{Y}T, quite strong fluorescent was observed for the ^{X}A–^{Y}G base pair. Based on the T_m increase, DANPH$^+$ bound to the C-bulge flanking both ^{X}C–^{Y}T and ^{X}A–^{Y}G. Therefore, the DANPH$^+$ fluorescence was modulated by the flanking mismatched base pairs. It is particularly noteworthy that the guanine in the ^{X}A–^{Y}G did not quench the fluorescence of the neighboring DANPH$^+$ bound to the C-bulge. While we do not have

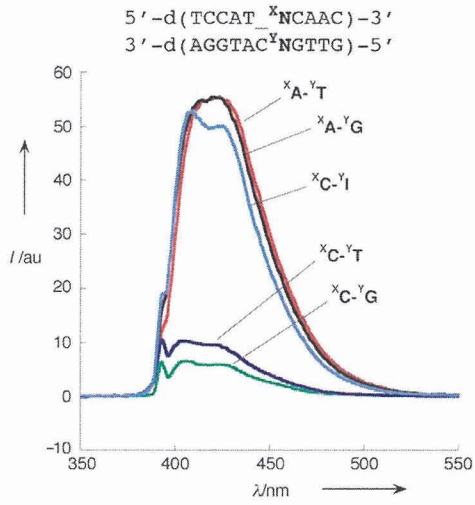

Figure 3. Fluorescence spectra of DANP (10 μM) was measured in the presence of C-bulge duplexes (50 μM) in a phosphate buffer (pH 7.0) and NaCl (100 mM). Excitation wavelength was 394 nm. ^{X}N–^{Y}N = A—T (red), A—G (black), C—T (blue), C–G (green), C—I (sky blue).

a rational explanation for these observations at this moment, this fluorescent property of DANPH$^+$ is worthy of future investigations.

Encouraged by the fluorescent measurements on selected matched and mismatched base pairs flanking the C-bulge, we have looked at the comprehensive survey of the effect of the flanking base pairs on the DANPH$^+$ fluorescence. Because the assay conditions with an excess amount of DNA are not feasible in practical SNP typing, the fluorescence measurements of DANPH$^+$ were investigated in the presence of a limited amount of C-bulge duplex. Since the absorption and emission spectra of the DANPH$^+$–C-bulge complex was shifted by 30 nm to a longer wavelength compared with those of unbound DANP, it was anticipated that we could selectively monitor the DANPH$^+$ bound to the C-bulge in the presence of unbound DANP. The DANPH$^+$ fluorescence was measured with 410 nm excitation and 460 nm emission filters to selectively monitor the DANPH$^+$-bound complex in the presence of unbound DANP (λ_{max} 365 nm). The observed fluorescence intensity (I_{obs}) in the presence of the C-bulge duplex is reported as a value (I_{rel}) relative to that of the background (I_{back}) measured without the C-bulge duplex.

There were two sequence motifs for the C-bulge probe in terms of the relative position of the C-bulge to the ^{X}N–^{Y}N base pair. The sequences 5′-A_^{X}N-3′/3′-T*C*^{Y}N-5′, 5′-T_^{X}N-3′/3′-A*C*^{Y}N-5′, and 5′-C_^{X}N-3′/3′-I*C*^{Y}N-5′ contained the bulged cytosine at the 3′ end of ^{Y}N, whereas other three sequences 5′-^{X}N_A-3′/3′-^{Y}N*C*T-5′, 5′-^{X}N_T-3′/3′-^{Y}N*C*A-5′, and 5′-^{X}N_C-3′/3′-^{Y}N*C*I-5′ contained the bulged cytosine at the 5′ end of ^{Y}N. The 5′-G_^{X}N-3′/3′-*C*C^{Y}N-5′ and 5′-^{X}N_G-3′/3′-^{Y}N*C*C-5′ sequence contained G at the 5′ or 3′ end of ^{X}N produced the I_{rel} to be 1 regardless to the ^{X}N–^{Y}N base pair and are not discussed here. The G flanking C-bulge in the probe was replaced with inosine to avoid fluorescence quenching by G.

The C-bulge in the first sequence series showed a common tendency of I_{rel} as representatively described for 5′-A_^{X}N-3′/3′-T*C*^{Y}N-5′(Table 2). Among 20 C-bulges in the sequence series of 5′-A_^{X}N-3′/3′-T*C*^{Y}N-5′, six C-bulges flanking ^{X}T–^{Y}A, ^{X}A–^{Y}A, ^{X}A–^{Y}T, ^{X}A–^{Y}G, ^{X}A–^{Y}I, and ^{X}C–^{Y}I showed the I_{rel} larger than 2. The largest I_{rel} was 4.2 for the

Table 2. I_{rel} of DANPH$^+$ bound to the C-bulge in the A_^{X}N/T*C*^{Y}N sequence.[a]

	5′-d(ACATCCAA_^{X}NCAACCAC)-3′ 3′-d(TGTAGGTTC^{Y}NGTTGGTG)-5′			
^{Y}N	^{X}N			
	T	A	G	C
^{Y}A	2.8	2.5	1.0	1.5
^{Y}T	1.4	3.5	0.9	1.2
^{Y}C	1.1	1.4	1.0	1.0
^{Y}G	1.4	3.1[b]	1.0	1.3
^{Y}I	1.9	4.2	1.1	2.8

[a] Fluorescence measurements were carried out for the solution containing 2 μM each of two C-bulge duplex and 50 μM DANP in a phosphate buffer (pH 7.0) and 100 mM NaCl. $I_{rel}=I_{obs}/I_{back}$. The error (s.e.m.) was 0.1 for three independent measurements unless otherwise noted. [b] The error was 0.2.

C-bulge flanking ^{X}A–^{Y}I. When the ^{X}N was guanine, the I_{rel} was nearly 1 regardless to the ^{Y}N. It was also characteristic that the I_{rel} was below 1.5 for the C-bulge containing C at either ^{X}N or ^{Y}N position. The only exception was the C-bulge flanking to ^{X}C–^{Y}I. The ^{X}A–^{Y}G mismatch produced a large I_{rel}. The data clearly show that the flanking sequence to the C-bulge had considerable effects on the DANPH$^+$ fluorescence bound to the C-bulge. Other two sequences 5′-T_^{X}N-3′/3′-A*C*^{Y}N-5′ (Table 3), and 5′-C_^{X}N-3′/3′-I*C*^{Y}N-5′ (Table 4) showed the similar I_{rel} values for a given ^{X}N–^{Y}N base pair.

Table 3. I_{rel} of DANPH$^+$ bound to the C-bulge in the T_^{X}N/AC^{Y}N sequence.[a]

	5′-d(ACATCCAT_^{X}NCAACCAC)-3′ 3′-d(TGTAGGTAC^{Y}NGTTGGTG)-5′			
^{Y}N	^{X}N			
	T	A	G	C
^{Y}A	2.6	2.6	0.9	1.3
^{Y}T	1.6	4.0	0.9	1.0
^{Y}C	1.2	1.5	0.9	1.0
^{Y}G	1.1	2.7	0.9	1.0
^{Y}I	2.1	3.7	1.0	2.3

[a] See Table 2.

In the second sequence series, where C-bulge was located at the 5′ end of the ^{Y}N, the I_{rel} was also sensitive to the flanking base pairs (Tables 5–7). When ^{X}N was G, the I_{rel} was almost 1 regardless to ^{Y}N as observed in the first sequence context. In contrast, the I_{rel} for the C-bulges containing ^{X}C was about two times higher than that observed in the first sequence context. This flanking base-pair dependency of the I_{rel} was common for the second sequence context. On

Table 4. I_{rel} of DANPH$^+$ bound to the C-bulge in the C_^{X}N/IC^{Y}N sequence.[a]

	5′-d(ACATCCAC_^{X}NCAACCAC)-3′ 3′-d(TGTAGGTIC^{Y}NGTTGGTG)-5′			
^{Y}N	^{X}N			
	T	A	G	C
^{Y}A	2.3	2.2	0.9	1.2
^{Y}T	1.5	3.3	0.9	1.2
^{Y}C	1.1	1.3	0.9	1.0
^{Y}G	1.2	3.0	0.9	1.0
^{Y}I	2.1	4.2	1.0	2.4

[a] See Table 2.

Table 5. I_{rel} of DANPH$^+$ bound to the C-bulge in the ^{X}N_A/^{Y}NCT sequence.[a]

	5′-d(ACATCCA^{X}N_ACAACCAC)-3′ 3′-d(TGTAGGT^{Y}NCTGTTGGTG)-5′			
^{Y}N	^{X}N			
	T	A	G	C
^{Y}A	4.0	3.0	1.0	1.9
^{Y}T	2.6	3.5	0.9	1.8
^{Y}C	2.0	2.5	1.0	1.8
^{Y}G	1.9	2.7	0.9	1.1
^{Y}I	2.4	4.8	0.9	3.3

[a] See Table 2.

the basis of these fluorescence measurements, the fluorescence of DANPH$^+$ bound to the C-bulge was selectively modulated by the ^{X}N–^{Y}N base pair directly neighboring 5′ and 3′ sides. The G directly flanking SNP site quenched the DANPH$^+$ fluorescence and thus did not allow fluorescence measurements. There were three sequence series regarding the position of G relative to ^{X}N; ^{X}N was flanked by 1) one G at the 5′ end (5′-G^{X}NN-3′), 2) one G at the 3′ end (5′-N^{X}NG-3′), and 3) two Gs at both 5′ and 3′ end (5′-G^{X}NG-3′). In the first two sequences, fluorescence quenching by G could be circumvented by the design of C-bulge probe. Thus, the position of the C-bulge was chosen such that the C-bulge was produced at the opposite side of the G as shown in Figure 4a and b. In the third sequence, a probe

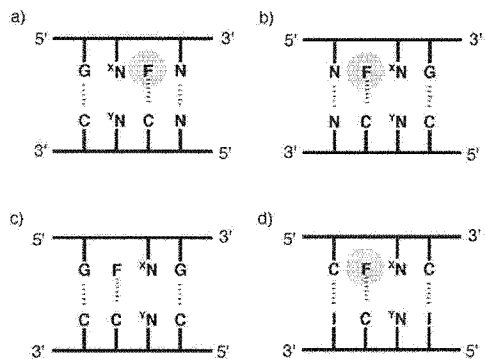

Figure 4. Discrimination of allelic types in six mutations with two C-bulge probes and DANP. Key: a) A to T; b) C to T; c) A to C; d) C to G; e) A to G; f) G to T mutations.

design was not effective to circumvent fluorescence quenching because C-bulge was always flanked by the G (Figure 4c). In this case, the fluorescence measurements should be done on the complementary strand in the 5′-C^{X}NC-3′ with the C-bulge probe having two inosine (I) opposite C (Figure 4d).

In the proposed SNP typing, the single-stranded DNA containing the SNP site was obtained by PCR followed by asymmetric PCR, then hybridized with the C-bulge probes. The DANP was added to the duplex and the fluorescence was measured. The fluorescence profiles of the given DNA sample regarding the C-bulge probes determined the SNP

Table 6. I_{rel} of DANPH$^+$ bound to the C-bulge in the ^{X}N_T/^{Y}NCA sequence.[a]

	5′-d(ACATCCA^{X}N_ACAACCAC)-3′ 3′-d(TGTAGGT^{Y}NCTGTTGGTG)-5′			
^{Y}N	^{X}N			
	T	A	G	C
^{Y}A	2.6	2.5	1.0	1.8
^{Y}T	2.3	2.8	1.0	1.9
^{Y}C	2.1	2.5	0.9	2.0
^{Y}G	1.3	1.7	0.9	1.0
^{Y}I	1.9	3.1	0.9	2.3

[a] See Table 2.

Table 7. I_{rel} of DANPH$^+$ bound to the C-bulge in the ^{X}N_C/^{X}NCI sequence.[a]

	5′-d(ACATCCA^{X}N_ACAACCAC)-3′ 3′-d(TGTAGGT^{Y}NCTGTTGGTG)-5′			
^{Y}N	^{X}N			
	T	A	G	C
^{Y}A	2.3	2.5	1.0	2.2
^{Y}T	1.9	2.8	0.9	2.3
^{Y}C	1.8	2.3	1.0	2.5
^{Y}G	1.3	1.7	0.9	1.0
^{Y}I	1.8	3.6	0.9	2.4

[a] See Table 2.

type. The SNP typing needs to discriminate three allelic types of wild type and mutant homozygotes and heterozygote. In homozygotes, the nucleotide base at the SNP site (^{X}N) is identical for two alleles, whereas a different base is found in each one of two alleles of heterozygotes. For example, in the A to C mutation, the homozygote of wild type has ^{X}A at the SNP site in two alleles (^{X}A/^{X}A), whereas the homozygote of mutant has ^{X}C in two alleles (^{X}C/^{X}C). The heterozygote has ^{X}A and ^{X}C at the SNP site in each allele (^{X}A/^{X}C). Six combinations of two bases (^{X}A/^{X}C, ^{X}A/^{X}G, ^{X}A/^{X}T, ^{X}C/^{X}G, ^{X}C/^{X}T, and ^{X}G/^{X}T) were correlated to the six types of single nucleotide mutations. The I_{rel} data shown in Tables 2–7 were obtained for the C-bulge flanked by one ^{X}N and indicated that the data were corresponding to those of homozygote samples.

The I_{rel} of heterozygote samples were measured for the DNA obtained by mixing two heterozygote samples. In Table 8, the I_{rel} data for the heterozygote samples in the 5′-A_^{X}N-3′/3′-TC^{Y}N-5′ sequence, where ^{X}N consisted of two

different nucleotide bases $^{X}N_1$ and $^{X}N_2$, is shown. The I_{rel} value was found to be the average of I_{rel} obtained for each one of two ^{X}N. This indicates that the binding of $DANPH^+$ to two different C-bulge duplexes is independent from each other under the conditions. With the I_{rel} profile of the homo- and heterozygote DNA against each one of C-bulge probes (Tables 2 and 8), the allelic type could be clearly discriminated by comparing the I_{rel} in terms of the ratio and the magnitude obtained for two C-bulge probes (Figure 5).

Table 8. I_{rel} of $DANPH^+$ bound to the C-bulge in heterozygote duplexes.[a]

	5′-d(ACATCCAA_$^{X}N_1$CAACCAC)-3′ 5′-d(ACATCCAA_$^{X}N_2$CAACCAC)-3′ 3′-d(TGTAGGTTC^{Y}NGTTGGTG)-5′					
^{Y}N	$^{X}N_1/^{X}N_2$					
	$^{X}A/^{X}C$	$^{X}A/^{X}G$	$^{X}A/^{X}T$	$^{X}C/^{X}G$	$^{X}C/^{X}T$	$^{X}G/^{X}T$
^{Y}A	2.0	1.7	2.6	1.2	2.1	1.9
^{Y}T	2.4	2.2	2.5	1.1	1.3	1.1
^{Y}C	1.2	1.2	1.2	1.0	1.1	1.0
^{Y}G	2.2	2.0[b]	2.3	1.1	1.3	1.2
^{Y}I	3.5[b]	2.7	3.2	2.0	2.4	1.5

[a] Fluorescence measurements were carried out for the solution containing 1 μM each of two 16 mer 5′-d(ACATCCAA$^{X}N_1$CAACCAC)-3′, 5′-d(ACATCCAA$^{X}N_2$CAACCAC)-3′ and 2 μM each of 17 mer 5′-(GTGGTTG^{Y}NCTTGGATGT)-3′ and 50 μM DANP in a phosphate buffer (pH 7.0) and 100 mM NaCl. $I_{rel}=I_{obs}/I_{back}$. The error (s.e.m.) was 0.1 for three independent measurements unless otherwise noted. [b] The error was 0.2.

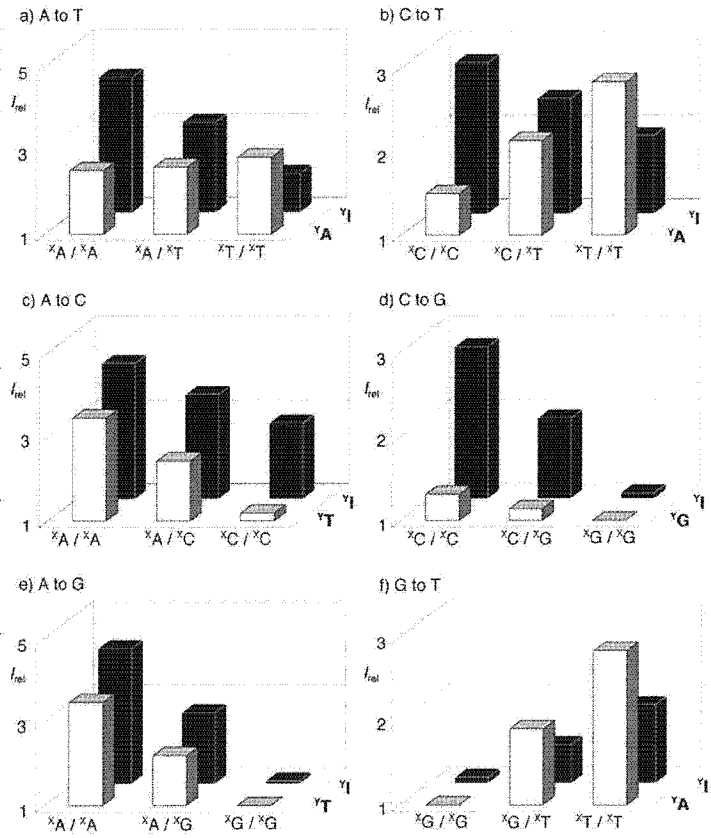

Figure 5. Selection of C-bulge probe with respect to the target sequence. a) C-bulge probe with the extra cytosine at the 5′ end of ^{Y}N; target: 5′-G^{X}NN-3′, probe: 5′-NC^{Y}NC-3′. b) C-Bulge probe with the extra cytosine at the 3′ side to ^{Y}N; target: 5′-N^{X}NG-3′, probe: 5′-C^{Y}NCN-3′. c) ^{X}N flanked by two G; target: 5′-G^{X}NG-3′, probe: 5′-C^{Y}NCC-3′. d) SNP typing should be done on the complementary strand having 5′-C^{X}NC-3′ sequence with the C-bulge contained two inosines; target: 5′-C^{X}NC-3′, probe: 5′-I^{Y}NCI-3′.

The allelic types in the A to T (or T to A) mutation were determined by two C-bulge probes containing ^{Y}A and ^{Y}I (Figure 5a). The C-bulge probe contained ^{Y}I was chosen instead of that containing ^{Y}T because the I_{rel} difference between ^{X}A and ^{X}T was larger for ^{Y}I than for ^{Y}T. Three allelic types of $^{X}A/^{X}A$, $^{X}A/^{X}T$, and $^{X}T/^{X}T$ produced a similar I_{rel} for the ^{Y}A-containing probe, but gave markedly different I_{rel} values for the ^{Y}I-containing probe. The ratio of I_{rel} obtained for the two C-bulge probes determined the allelic type. In the C to T (or T to C) and A to C (or C to A) mutations (Figure 5b and c), the allelic type could be also determined by the ratio metric analysis. The other three mutations of G to N (N = A, T, and C) could be analyzed by the difference in the intensity of I_{rel} for each of the C-bulge probes used for the analysis. Because the $^{X}G/^{X}G$ homozygote showed an I_{rel} of 1.0, the I_{rel} of the heterozygote ($^{X}G/^{X}N$) would be one half of that obtained for $^{X}N/^{X}N$ homozygote DNA. For a practical applicability, the predetermined profile of I_{rel} for the allelic type could be used as a standard for the diagnosis of testing samples.

Conclusion

The SNP-typing method described here exploits the C-bulge as a scaffold to recruit and keep DANP directly neighboring the SNP site. The method does not require covalent modification of the probe DNA and uses only one fluorescent molecule, that is, DANP, for the assay. The high flexibility in the probe design is another characteristic of the proposed SNP typing and makes the method applicable in principle to any target sequence. Especially, the fluorescence quenching by G could be circumvent by probe design and the effective use of inosine in the probe. However, bulge binding molecules with improved fluorescence properties, stronger fluorescence intensity, a large absorption and emission shift upon binding to C-bulge, and a large fluorescence difference with neighboring base pairs are necessary for this proposed method to be applicable for SNP typing. It is also important to understand the chemical basis that the $DANPH^+$–C bulge complex neighboring ^{X}A–^{Y}G, ^{X}C–^{Y}I and ^{X}A–^{Y}I base pairs emitted strong fluorescence. These studies may provide a way to avoid the fluorescence quenching by ^{X}G.

Experimental Section

Measurements of melting temperature of bulge-containing duplexes: DANP (50 μM) was dissolved in a sodium cacodylate (10 mM, pH 7.0) containing bulge duplex (2 μM) and NaCl (100 mM). The thermal denaturation profile was recorded on a Shimadzu UV2550 spectrometer equipped with a Shimadzu TMSPC-8 temperature controller. The absorbance of the sample was monitored at 260 nm from 4 °C to 80 °C with a sample heating rate of 1 °C min^{-1}.

UV and fluorescent spectra measurements: UV spectra were recorded on a Shimadzu UV2550 spectrometer. Fluorescent spectra were recorded on a Shimadzu RF-5300PC. DNA samples were prepared in 10 mM sodium phosphate buffer at the designated pH 7.0 in the presence of 100 mM sodium chloride. Excitation wavelength for the fluorescent measurements was the wavelength at the absorption maximum unless otherwise noted. The fluorescence intensity was recorded on a Berthold Mithras LB 940 with 410 nm excitation and 460 nm emission filters. The measurements were carried out for the solution containing 2 μM each of two C-bulge duplex and 50 μM of DANP on the phosphate buffer (pH 7.0) and 100 mM NaCl.

Acknowledgements

This work was supported by a Grant-in-Aid for Scientific Research (C) from Japan Science for the Promotion of Science and Health and Labour Sciences Research Grants for Research on Advanced Medical Technology from the Ministry of Health, Labour and Welfare.

[1] P. Y. Kwok, *Annu. Rev. Genomics Hum. Genet.* **2001**, *2*, 235.
[2] A.-C. Syvänen, *Nat. Rev. Genet.* **2001**, *2*, 930.
[3] J. Tost, V. G. Gut, *Mass Spectrom. Rev.* **2002**, *21*, 388.
[4] T. G. Drummond, M. G. Hill, J. K. Barton, *Nat. Biotechnol.* **2003**, *21*, 1192.
[5] K. Nakatani, *ChemBioChem* **2004**, *5*, 1623.
[6] M. Strerath, A. Marx, *Angew. Chem.* **2005**, *117*, 8052; *Angew. Chem. Int. Ed.* **2005**, *44*, 7842.
[7] A. Okamoto, Y. Saito, I. Saito, *J. Photochem. Photobiol. C* **2005**, *6*, 108.
[8] A. Yamane, *Nucleic Acids Res.* **2002**, *30*, e97.
[9] G. T. Hwang, Y. J. Seo, B. H. Kim, *J. Am. Chem. Soc.* **2004**, *126*, 6528.
[10] Y. J. Seo, J. H. Ryu, B. H. Kim, *Org. Lett.* **2005**, *7*, 4931.
[11] K. Yamana, Y. Fukunaga, Y. Ohtani, S. Sato, M. Nakamura, W. J. Kim, T. Akaike, A. Maruyama, *Chem. Commun.* **2005**, 2509.
[12] O. Köhler, D. V. Jarikote, O. Seitz, *ChemBioChem* **2005**, *6*, 69.
[13] A. P. Silverman, E. T. Kool, *Nucleic Acids Res.* **2005**, *33*, 4978.
[14] L. Valis, N. Amann, H.-A. Wagenknecht, *Org. Biomol. Chem.* **2005**, *3*, 36.
[15] A. Okamoto, K. Kanatani, I. Saito, *J. Am. Chem. Soc.* **2004**, *126*, 4820.
[16] Y. Saito, Y. Miyauchi, A. Okamoto, I. Saito, *Chem. Commun.* **2004**, 1704.
[17] C. Dohno, I. Saito, *ChemBioChem* **2005**, *6*, 1075.
[18] K. Yoshimoto, C.-Y. Xu, S. Nishizawa, T. Haga, H. Satake, N. Teramae, *Chem. Commun.* **2003**, 2960.
[19] K. Yoshimoto, S. Nishizawa, M. Minagawa, N. Teramae, *J. Am. Chem. Soc.* **2003**, *125*, 8982.
[20] H. Suda, A. Kobori, J. Zhang, G. Hayashi, K. Nakatani, *Bioorg. Med. Chem.* **2005**, *13*, 4507.
[21] A. O. Crockett, C. T. Wittwer, *Anal. Biochem.* **2001**, *290*, 89.
[22] C. A. M. Seide, A. Schulz, M. H. M. Sauer, *J. Phys. Chem.* **1996**, *100*, 5541.

Received: October 20, 2006
Revised: November 30, 2006
Published online: ■■ ■■, 2007

A recruiting scaffold: The probe DNA provides a C-bulge as a scaffold to recognize and retain the fluorescent molecule DANP (*N*,*N*′-bis(3-aminopropyl)-2,7-diamino-1,8-naphthyridine, denoted as F) directly neighboring the single nucleotide polymorphism site at ^{X}N. The DANP fluorescent probe was selectively modulated by the flanking ^{X}N–^{Y}N base pair, thus reporting the type of mutation.

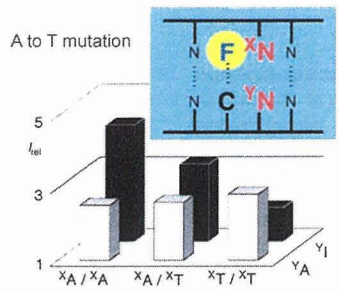

DNA Base Pairing

*F. Takei, H. Suda, M. Hagihara, J. Zhang, A. Kobori, K. Nakatani** ..... ▮▮▮▮–▮▮▮▮

Allele Specific C-Bulge Probes with One Unique Fluorescent Molecule Discriminate the Single Nucleotide Polymorphism in DNA

Anal. Chem. **2007**, *79*, 2552−2555

Exploiting Small Molecule Binding to DNA for the Detection of Single-Nucleotide Mismatches and Their Base Environment

Xiaohong Li,† Haifeng Song,† Kazuhiko Nakatani,‡ and Heinz-Bernhard Kraatz*,†

Department of Chemistry, University of Saskatchewan, 110 Science Place, Saskatoon, Saskatchewan, S7N 5C9, Canada, and Department of Regulatory Bioorganic Chemistry, The Institute of Scientific and Industrial Research (SANKEN), Osaka University, Ibaraki 567-0047, Japan

Naphthyridine−azaquinolone (Npt−Azq, described previously by Nakatani et al. (Nakatani, K.; Hagihara, S.; Goto, Y.; Kobori, A.; Hagihara, M.; Hayashi, G.; Kyo, M.; Nomura, M.; Mishima, M.; Kojima, C. *Nat. Chem. Biol.* 2005, *1*, 39−43.), was exploited to detect an adenine−adenine mismatch with a symmetrical G−C flanking sequence (5′-GAC-3′/5′-CAG-3′) in a synthetic 20-mer DNA by electrochemical impedance spectroscopy. This innovative strategy enables us to obtain information about the presence of a specific mismatch in addition to sequence information. Npt−Azq binds the G−A region of the mismatch, which causes significant changes in the structure of the DNA, which in turn causes changes in the electrochemical properties of DNA/Npt−Azq films. For a 20-mer DNA containing an A−A mismatch, the electron-transfer resistance (R_{CT}) of the system is significantly different in the presence of bound Npt−Azq, presumably due to the structural differences in the two films. Npt−Azq does not bind to matched DNA, and thus, the presence of Npt−Azq does not affect the electrochemical properties of such films.

Charge transport through DNA is sensitive to slight variation in the base pair π-stacking,[1−3] DNA sequence, and its structure.[4] Monitoring charge transport has allowed the development of a series of sensitive assays for the detection of base-stack perturbations, including mismatches.[1−3] Electrochemical mismatch detection often relies on the presence of probe molecules. Intercalators, such as daunomycin[1] and methylene blue,[2] chemically attached molecules, such as ferrocene,[5] and solution-based probes such as $[Fe(CN)_6]^{3-/4-}$ [6] have been employed.

Optical methods also have made significant contributions for the detection of mismatches.[7−15] Recently, the small molecular ligand, naphthyridine-azaquinolone (Npt−Azq) was employed to detect guanine−adenine (G−A) mismatches by surface plasmon resonance.[16] It was shown that Npt−Azq strongly interacts with G−A through hydrogen bonding and that the region flanking the mismatch is crucial for the molecular recognition. On the basis of this binding ability, Npt−Azq was used to study $(CAG)_n$ trinucleotide repeats.[17] It was shown that two Npt−Azq molecules can bind to a A−A mismatch and to the neighboring 3′-Gs in the CAG/CAG sequence. The two bases bind with one Npt−Azq molecule through complementary hydrogen bonding. As a result, a cytidine (C) nucleotide was induced to extrude from the hairpin structure. Thus, base pair π-stacking is strongly influenced, causing a large chiral change in the DNA duplex, which manifests itself in the CD spectrum of the duplex. As a result, one may expect that the electronic properties of the DNA will change too. It is important to point out that this molecule provides more than just information about the presence of a particular mismatch. In essence it also provides some information about the immediate base pair environment of the mismatch and thus gives sequence information. There are of course a large number of reports available dealing with the sequence-specific interactions of small

* To whom correspondence should be addressed. E-mail: kraatz@skyway.usask.ca.

† University of Saskatchewan.

‡ Osaka University.

(1) Kelley, S. O.; Boon, E. M.; Barton, J. K.; Jackson, N. M.; Hill, M. G. *Nucleic Acids Res.* **1999**, *27*, 4830−4837.

(2) Boon, E. M.; Ceres, D. M.; Drummond, T. G.; Hill, M. G.; Barton, J. K. *Nat. Biotechnol.* **2000**, *18*, 1096−1100.

(3) Boal, A. K.; Barton, J. K. *Bioconjugate Chem.* **2005**, *16*, 312−321

(4) Shao, F.; Augustyn, K.; Barton, J. K. *J. Am. Chem. Soc.* **2005**, *127*, 17445−17452.

(5) Yu, C. J.; Wan, Y. J.; Yowanto, H.; Li, J.; Tao, C. L.; James, M. D.; Tan, C. L.; Blackburn, G. F.; Meade, T. J. *J. Am. Chem. Soc.* **2001**, *123*, 11155−11161.

(6) Li, X. H.; Zhou, Y. L.; Sutherland, T. C.; Baker, B.; Lee, J. S.; Kraatz, H. B. *Anal. Chem.* **2005**, *77*, 5766−5769.

(7) Skogerboe, K. J. *Anal. Chem.* **1995**, *67*, 449R−454R.

(8) Wagner, R.; Debbie, P.; Radman, M. *Nucleic Acids Res.* **1995**, *11*, 3944−3948.

(9) Jain, K. K. *Science* **2001**, *294*, 621−623

(10) Afanassiev, V.; Hanemann, V.; Wolfl, S. *Nucleic Acids Res.* **2000**, *28*, e66.

(11) Proundnikov, D.; Timofeev, E.; Mirzabekov, A. *Anal. Biochem.* **1998**, *259*, 34−41.

(12) Ferguson, J. A.; Steemers, F. J.; Walt, D. R. *Anal. Chem.* **2000**, *72*, 5618−5624.

(13) Ali, M. F.; Kirby, R.; Goodey, A. P.; Rodriguez, M. D.; Ellington, A. D.; Neikirk, D. P.; McDevitt, J. T. *Anal. Chem.* **2003**, *75*, 4732−4739.

(14) Behrensdorf, H. A.; Pignot, M.; Windhab, N.; Kappel A. *Nucleic Acids Res.* **2002**, *30*, e64.

(15) Bi, L.-J.; Zhou, Y. F.; Zhang, J.-Y.; Zhang, Z.-P.; Xie, B.; Zhang, C.-G. *Anal. Chem.* **2003**, *75*, 4113−4119.

(16) Hagihara, S.; Kumasawa, H.; Goto, Y.; Hayashi, G.; Kobori, A.; Saito, I.; Nakatani, K. *Nucleic Acids Res.* **2004**, *32*, 278−286.

(17) Nakatani, K.; Hagihara, S.; Goto, Y.; Kobori, A.; Hagihara, M.; Hayashi, G.; Kyo, M.; Nomura, M.; Mishima, M.; Kojima, C. *Nat. Chem. Biol.* **2005**, *1*, 39−43.

10.1021/ac0615504 CCC: $37.00
Published on Web 02/06/2007

Chart 1. Small Molecular Ligand: Naphthyridine–Azaquinolone (Npt–Azq)

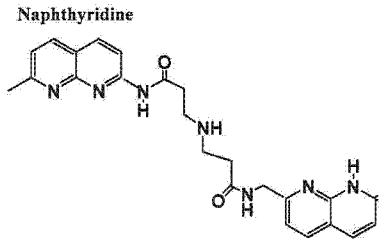

molecules with DNA. In these studies, the interaction was quantified using optical techniques.[18–20]

We set out to explore the feasibility of monitoring binding of a sequence-specific small molecule to DNA by electrochemical methods. In this study, a synthetic 20-mer DNA duplex containing a CAG/CAG unit was used to form an adenine–adenine mismatch. This mismatch is flanked by a region that allows effective binding to Npt–Azq. Electrochemical impedance spectroscopy (EIS) was used to evaluate binding of Npt–Azq to films of matched and mismatched DNA on gold. Previously we have shown that the charge-transfer resistance R_{CT} in DNA films is a useful parameter that, when compared to mismatched DNA films, allows us to determine the presence of a single-nucleotide mismatch.[6] If we can successfully detect binding of Npt–Azq to DNA, this would provide additional sequence information about the mismatch. To our knowledge, there are at present no electrochemical techniques available that provide information about the DNA sequence.

EXPERIMENTAL SECTION

Materials. Three DNA sequences were synthesized by standard solid-phase techniques using a fully automated DNA synthesizer at the Plant Biotechnology Institute (PBI-NRC, Saskatoon, SK, Canada).

1: HO-$(CH_2)_6$-SS-$(CH_2)_6$-5′-GTC-ACG-ATG-GCC-CAG-TAG-TT-3′

2: 3′-CAG-TGC-TAC-CGG-GTC-ATC-AA-5′

3: 3′-CAG-TGC-TAC-CGG-GAC-ATC-AA-5′

The characterization and purification of the DNA sequences were performed by two-step, reversed-phase HPLC and MALDI-TOF MS.

$NaClO_4$, $K_3[Fe(CN)_6]$, and $K_4[Fe(CN)_6]$ were purchased from Aldrich and used without further purification. Tris-ClO_4 were purchased from Fluka Co. Deionized water (18.2 MΩ·cm resistivity) from a Millipore Milli-Q system was used throughout this work.

N-Boc-Npt–Azq was used as reported before. The Boc group was removed by a reported procedure.[16] Prehybridized double-stranded DNA (ds-DNA) solutions (1 + 2 giving matched DNA **I** and 1 + 3 giving A–A mismatched DNA **II**) was prepared (1×10^{-4} M DNA in 50 mM Tris-ClO_4 buffer at pH 7.0). Npt–Azq was dissolved in 50 mM Tris-ClO_4 (pH 7.0, $c = 5 \times 10^{-5}$ M). This solution is then interacted with matched (**I**) or mismatched (**II**) DNA at Npt–Azq concentrations ranging from 5×10^{-5} to 5×10^{-9} M. The DNA concentration was kept constant at 1×10^{-5} M. DNA films were prepared by incubating gold microelectrodes (10 μm) for 5 days.

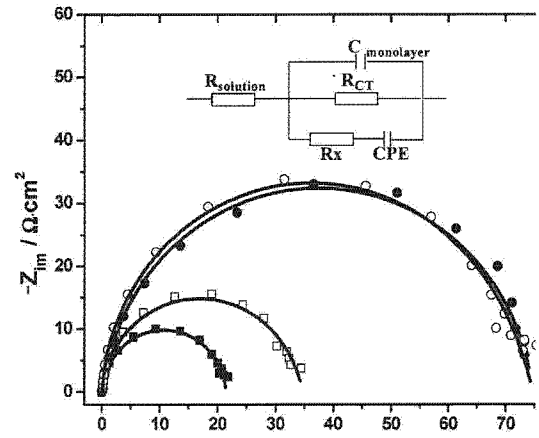

Figure 1. Typical Nyquist plots ($-Z_{im}$ vs Z_{re}) of the 20-base pair matched DNA **I** (●), **I** + Npt–Azq (○), **II** (■), and **III** (□). Measured data are shown as symbols with the fitting to the equivalent circuit as solid lines. Inset: the measured data are fit to the equivalent circuit as R_s, solution resistance; $C_{monolayer}$, capacitance of monolayer; R_{CT}, charge-transfer resistance; R_x and CPE, defects in the monolayer. The fitting data are summarized in Table 1.

Electrochemical Measurements. All measurements were carried out at room temperature (22 °C) in an enclosed and grounded Faraday cage. A conventional three-electrode system was used: a DNA modified gold microelectrode as working electrode, a Ag/AgCl/3M NaCl as reference work, and a platinum wire as counter electrode. The Ag/AgCl reference electrode, was connected to a 4 mM solution of $[Fe(CN)_6]^{3-/4-}$ in 50 mM Tris-ClO_4 buffer at pH 7.0 through a miniature salt bridge (agar plus KNO_3). EIS was measured using an EG&G 1025 frequency response analyzer interfaced to an EG&G 283 potentiostat/galvanostat. The ac voltage amplitude is 10 mV, and the voltage frequencies range from 100 kHz to 0.1 Hz. The applied potential was 250 mV versus Ag/AgCl (formal potential of the redox probe $[Fe(CN)_6]^{3-/4-}$ in the buffer solution). Importantly, all measurements were repeated for 10 electrodes to get statistically meaningful results.

RESULTS AND DISCUSSION

It has been shown that the small molecular DNA ligand, Npt–Azq, shown in Chart 1, can selectively and strongly bind to G–A through hydrogen bonding. The two parts of the molecule recognize different bases. Npt, 2-amino-1,8-naphthyridine, has three complementary hydrogen bonds that bind to G, while Azq, 8-azaquinolone, has two complementary hydrogen bonds that bind to A.[16] Solution spectroscopic studies were carried out to investigate the solution interaction of Npt–Azq with matched ds-DNA (1 + 2, **I**) and with mismatched ds-DNA (1 + 3, **II**) and are summarized in the Supporting Information (Figures S1 and S2).

(18) Dervan, Peter B. *Bioorg. Med. Chem.* **2001**, *9*, 2215–2235.
(19) Rucker, V. C.; Dunn, A. R.; Sharma, S.; Dervan, P. B.; Gray, H. B. *J. Phys. Chem. B* **2004**, *108*, 7490–7494.
(20) Kwon, Youngjoo.; Arndt, H–D.; Mao, Q.; Choi, Y.; Kawazoe, Y.; Dervan, P. B.; Uesugi, M. *J. Am. Chem. Soc.* **2004**, *126*, 15940–15941.

Chart 2. Schematic Representation of the DNA Conformation Change Induced by Npt–Azq: (I) Matched DNA (strands 1 + 2), (II) A–A Mismatched DNA (strands 1 + 3), and (III) A–A Mismatched DNA (1 + 3) Binding with Npt–Azq

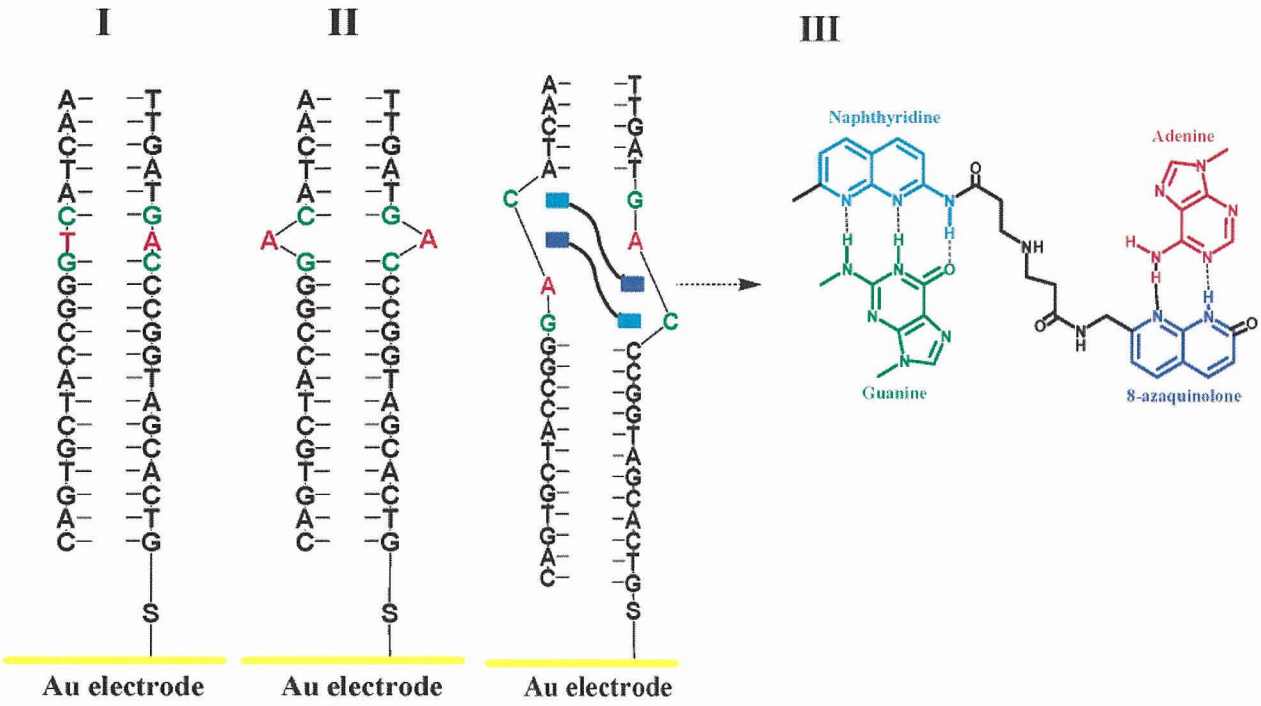

Table 1. Equivalent Circuit Element Values for DNA Films Prepared from Matched ds-DNA (I) and A–A Mismatched DNA (II) in the Presence and Absence of Npt–Azq[a]

film	R_s (Ω·cm^2)	$C_{monolayer}$ (μF cm^{-2})	R_{CT} (Ω·cm^2)	R_x (Ω·cm^2)	CPE (mF·cm^{-2})	n
I	0.01	95.5 (9.1)	74.1 (5.3)	0.1 (0.02)	3.6 (0.4)	0.8(0.02)
I + Npt–Azq	0.01	94.9 (9.1)	74.2 (5.3)	0.1 (0.02)	3.5 (0.4)	0.8(0.02)
II	0.01	105.8 (11.1)	22.0 (2.1)	0.1 (0.02)	4.5 (0.5)	0.8(0.01)
III	0.01	99.5 (9.8)	33.7 (2.9)	0.1 (0.03)	6.8 (0.7)	0.8(0.02)

[a] The values in parentheses represent the standard deviations from several electrode measurements ($n \geq 10$).

Our circular dichroism studies show that structural changes occur upon binding of Npt–Azq to mismatched DNA containing the A–A mismatch in a symmetric C–G flanking region.

Prehybridized ds-DNA was prepared as described in the Experimental Section, using matched DNA **I**, prepared by the combination of strands 1 + 2 and A–A mismatched DNA **II**, prepared by the combination of strands 1 + 3. The concentrations of the ds-DNA **I** and **II** were adjusted to 1×10^{-5} M with 50 mM Tris-ClO_4 (pH 7). Npt–Azq (5×10^{-5} M) was then added to both solutions. After incubation, DNA films were prepared on 10-μm gold electrodes exploiting the disulfide linker at the 5′-terminal side of strand 1 as shown in Chart 2. The electrochemical properties of these DNA films in the presence of $[Fe(CN)_6]^{3-/4-}$ were evaluated by EIS. Typical impedance spectra for the assembled DNA films are shown in Figure 1. These spectra are analyzed with the help of a modified Randles' equivalent circuit, as shown in the inset of Figure 1. The equivalent circuit compares well with that reported before for DNA films on 10-μm electrodes.[6]

R_s, 0.01 Ω·cm^2, is the solution resistance, which is a resistance between Ag/AgCl reference electrode and gold working electrode. $C_{monolayer}$ is used to account for DNA film capacitance. In the process of self-assembly, some defects in the films are unavoidable. The combination of R_x and a constant-phase element (CPE) accounts for possible defects in the DNA films. In addition, CPE is a nonlinear capacitor indicating inhomogeneity on the electrode surface.[21] Under our conditions, R_x (0.1 Ω·cm^2) is much smaller than R_{CT} (0.7 Ω·cm^2) for the bare electrode, which indicates that the resistance of the defect sites is small. A comparison of R_{CT} and R_x for the assembled films indicates that more homogeneous DNA films are formed on the microelectrode compared to bigger electrode (diameter, 2 mm).[22] A diffusive element that would account for the diffusion of the redox probe $[Fe(CN)_6]^{3-/4-}$ from the bulk solution to the DNA film is negligible in this system because of the absence of any Warburg impedance as shown in Figure 1.

(21) Dijkama, M.; Boukamp, B. A.; Kamp, B.; van Bennekom, W. P. *Langmuir* **2002**, *18*,3105–3112.
(22) Long, Y. T.; Li, C. Z.; Sutherland, T. C.; Kraatz, H. B.; Lee, J. S. *Anal. Chem.* **2004**, *76*, 4059–4065.

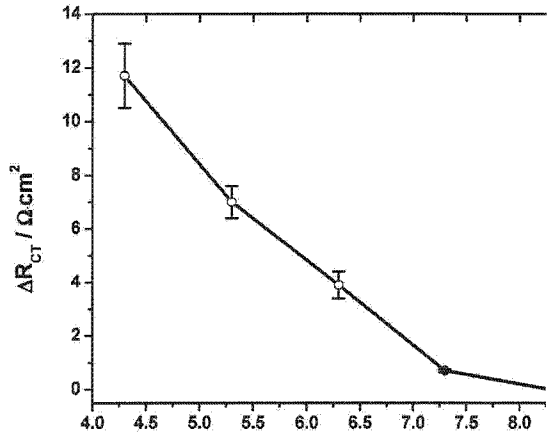

Figure 2. Relationship between ΔR_{CT} and the concentration of Npt–Azq.

The electron-transfer resistance R_{CT} is a resultant resistance accounting for the resistance of charge transfer from the $[Fe(CN)_6]^{3-/4-}$ redox probe to the electrode surface through the DNA film. For the matched ds-DNA **I**, R_{CT} is 74.1 (5.3) Ω·cm^2. For the mismatched ds-DNA **II** containing an A–A mismatch, the R_{CT} is 22.0 (2.1) Ω·cm^2. After binding of ds-DNA **II** with Npt–Azq to form the adduct **III**, R_{CT} increased to 33.7 (2.9) Ω·cm^2. Since the ligand does not bind to fully matched DNA, the addition of Npt–Azq to the matched ds-DNA **I** had no effect on the R_{CT} of the film. The explanation of the sensitivity for the mismatch in this system is provided by a simple electrostatic argument. The negatively charged $[Fe(CN)_6]^{3-/4-}$ redox probe is electrostatically repelled by negatively charged phosphates on DNA and cannot penetrate the film for a well-formed film of ds-DNA. Films that do not contain a mismatch should be better packed, while those containing a mismatch will be more disordered due to structural changes that can occur in the ds-DNA. Repulsion between the ds-DNA and the anionic redox probe is enhanced for a well-packed film; thus, R_{CT} should be higher. Following the same argument, a mismatched film containing, for example, an A–A mismatch, is presumably less tightly packed or more disordered, which allows the redox probe to penetrate the film more, resulting in a lower R_{CT}.

It is interesting to note that, after binding of Npt–Azq to a mismatched ds-DNA to form the adduct **III** as shown in Chart 2, the R_{CT} increases reproducibly from 22.0 (2.1) to 33.7 (2.9) Ω·cm^2. This suggests that the DNA film for the adduct **III** is more ordered and charge penetration is more difficult compared to films of the mismatched film of ds-DNA **II**. It is known from previous work that the Npt and Azq parts of the ligand form hydrogen bonds with guanine and adenine, respectively, showing Watson–Crick-like pairing. This will cause flipping of the cytidine out of the duplex.[17] For a mismatched film, this may in fact have dramatic consequences, making the film more rigid possibly due to the potential addition H-bonding among the flipped cytidines.

Next, we evaluated the concentration dependence. How much Npt–Azq is necessary to enable us to see an effect by EIS? In order to answer this question, we carried out dilution studies. The concentration of ds-DNA **II** was kept constant at 1×10^{-5} M, while the concentration of the ligand Npt–Azq in the solutions was varied from 5×10^{-5} to 5×10^{-9} M. As a result, films of **III** are expected to contain different amounts of Npt–Azq adducts. We monitored the difference in charge-transfer resistances ΔR_{CT} between films of the mismatched ds-DNA **II** and the adduct **III**. The relationship between ΔR_{CT} and the concentration of Npt–Azq is shown in Figure 2. We observed a virtually linear relationship between ΔR_{CT} and the concentration of Npt–Azq in the range of 5×10^{-5}–5×10^{-8} M. At a concentration of 5×10^{-9} M in Npt–Azq, there is no discernible difference between the R_{CT} for mismatched ds-DNA in the absence (**II**) and presence of the ligand Npt–Azq (**III**). Initial EIS studies of DNA films involving other mismatches (CGG/GAC and CGG/GGC) did not show significant differences in the absence and presence of Npt–Azq that would be indicative of binding.

CONCLUSION

Binding of a synthetic 20-mer DNA with the sequence-specific ligand naphthyridine–azaquinolone causes significant electrochemical effects in the ds-DNA possessing an A–A mismatch that is flanked by C–G/C–G sequences. We established the difference in the charge-transfer resistance ΔR_{CT} between films of the mismatched ds-DNA **II** and the adduct **III** as a measure that enables us to detect the bound ligand. While the ligand does not bind to matched DNA, it binds selectively to the A–A mismatched DNA **II** resulting in a ΔR_{CT} of 11. 7 (2.9) Ω·cm^2. Thus, for the first time, we were able to demonstrate the use of EIS of ds-DNA films to provide not just information about the presence of a single-nucleotide mismatch but are now able to provide base sequence information that previously was not accessible by simple electrochemical measurements.

ACKNOWLEDGMENT

This work was supported by funding through the NSERC Strategic program. H.-B.K is the Canadian Research Chair in Biomaterials. The authors also thank Don Schwab, the Plant Biotechnology Institute, Canada, for the preparation of DNA samples.

SUPPORTING INFORMATION AVAILABLE

Additional information as noted in text. This material is available free of charge via the Internet at http://pubs.acs.org.

Received for review August 18, 2006. Accepted December 19, 2006.

AC0615504

DOI: 10.1002/cbic.200600564

Small-Molecule Binding to the Nonquadruplex Form of the Human Telomeric Sequence

Yuki Goto,[a] Shinya Hagihara,[a] Masaki Hagihara,[a, b] and Kazuhiko Nakatani*[a, b]

The telomeric sequence d(TTAGGG)$_n$ located at the 3′ end of human genomic DNA plays important roles in protecting chromosomal ends from fusion, rearrangement, and translocation.[1,2] In normal cells, the entire length of the telomere gradually decreases as the replication of the genome is repeated,[3,4] due to the inability of DNA polymerase to replicate the extreme 3′ end of the template. In contrast, the enzyme telomerase is activated in the nuclei of cancer cells and maintains the length of the telomere so as to achieve immortality.[5] Therefore, ligands that bind to telomeres and inhibit their elongation are expected to be potential anticancer drugs.[6–10] The single-stranded region of the d(TTAGGG)$_n$ repeat is known to form G-quadruplex structures in vitro,[11–15] and a number of molecular ligands that bind to and strengthen the G-quadruplex structure have been investigated.[16–24]

We have taken an alternative approach to molecules binding to the telomeric sequence. Naphthyridine dimer (ND) binds to the G–G mismatch[25,26] in duplex DNA bound to the human telomeric sequence.[27] CD measurements showed that the structure of the G-quadruplex of d(AGGGTTAGGGTTAGGGTTAGGGTTA) changed upon ND binding. While we have studied the mode of ND binding to the telomeric sequence, no conclusive result was obtained, because the stoichiometry of the ND binding to the model sequence d(TTAGGGTTAGGGTTA) (telo15) of human telomere was not unique. We here report a new molecule, naphthyridine tetramer (NT), that binds to telo15 with an exclusive 1:1 binding stoichiometry. From ESI-TOF MS and UV melting profiles of telo15 mutants, it was suggested that NT bound to the two of the three G–G mismatches in the hairpin secondary structure.

NT was synthesized by a successive reductive amination of ND with glutaraldehyde. The binding of NT to the telomeric sequence, especially the binding stoichiometry, was evaluated by ESI-TOF MS (Figure 1).[28] ESI-TOF MS of telo15 showed a 4^- ion (*m/z* 1168.92) and a 3^- ion (*m/z* 1558.83) of a monomer, and a 5^- ion (*m/z* 1871.11) corresponding to a telo15 dimer, which

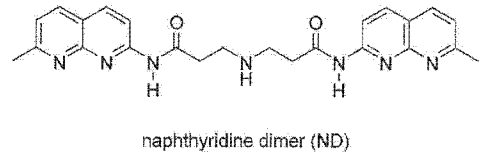

naphthyridine dimer (ND)

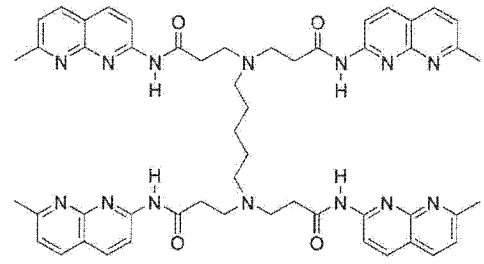

naphthyridine tetramer (NT)

was most likely an interstrand G-quadruplex. These ion peaks decreased in intensity in the presence of NT, with a concomitant appearance of a distinct ion at *m/z* 1407.71, which corresponded to the 4^- ion of a 1:1 complex of NT with telo15 ([telo15+NT]$^{4-}$). No other ions corresponding to complexes with a different binding stoichiometry or any ion of NT complexes bound to the telo15 dimer could be detected, even at a high NT concentration (60 μM). To gain an insight into the mode of NT binding to telo15, ESI-MS was performed on a mutant sequence of telo15—d(TTAZZZTTAZZZTTA) (telo15Z)—in which all of the guanine bases (G) were substituted by 7-

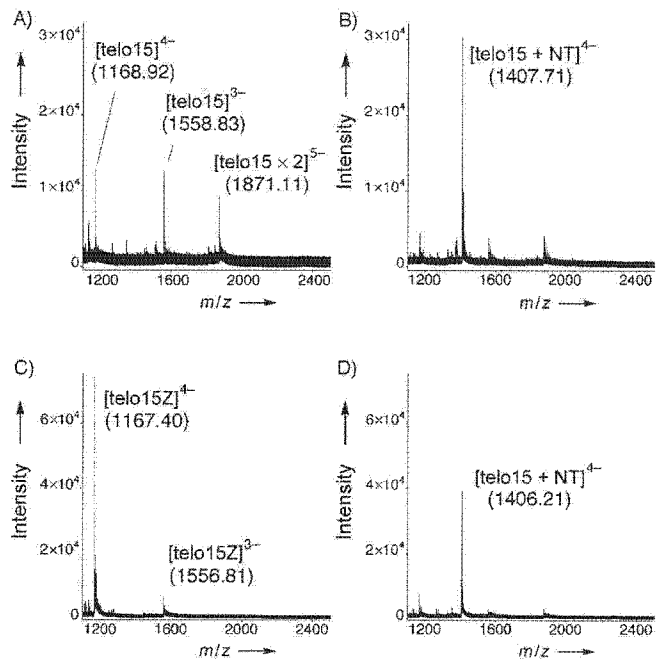

Figure 1. The ESI-TOF MS of telo15 and telo15Z with NT. The spectra were obtained in 50% aqueous methanol and 100 mM NH_4OAc. A) telo15 (20 μM), B) telo15 (20 μM) and NT (20 μM), C) telo15Z (20 μM), and D) telo15Z (20 μM) and NT (20 μM).

[a] *Y. Goto, Dr. S. Hagihara, Dr. M. Hagihara, Prof. Dr. K. Nakatani*
Department of Synthetic Chemistry and Biological Chemistry
Graduate School of Engineering, Kyoto University
Kyoto 615-8510 (Japan)

[b] *Dr. M. Hagihara, Prof. Dr. K. Nakatani*
Current address: Department of Regulatory Bioorganic Chemistry
The Institute of Scientific and Industrial Research, Osaka University
8–1 Mihogaoka, Ibaraki 567-0047 (Japan)
Fax: (+81) 6-6879-8459
E-mail: nakatani@sanken.osaka-u.ac.jp

Supporting information for this article is available on the WWW under http://www.chembiochem.org or from the author.

deazaguanine (Z), that is the N7 of G was replaced with CH. As shown in Scheme 1A, the G-quadruplex structure consists of two kinds of hydrogen bond; one is between the N1-H and C6 carbonyl oxygen, and the other is between the hydrogen in

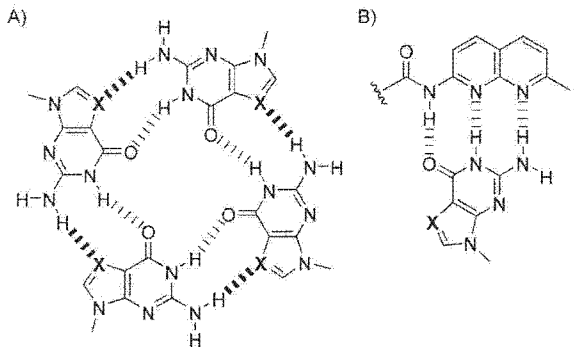

Scheme 1. A) Structure of the G-quadruplex with X = N. 7-Deazaguanine (X = CH) cannot form a quadruplex due to the lack of hydrogen bonding to the 2-amino group (shown with a bold dash). B) Hydrogen bonding of *N*-acyl-2-amino-1,8-naphthyridine in **NT** to guanine (X = N) and 7-deazaguanine (X = CH).

the N2 amino group and N7. A loss of the NH_2···N7 hydrogen bonds from substituting G with Z and a potential steric repulsion between NH_2 and C7-H in a hypothetical Z-quadruplex suggests that formation of a quadruplex structure of telo15Z would be unlikely. In fact, ESI-TOF MS showed that telo15Z did not produce a dimer under the conditions given in Figure 1C. However, a 1:1 complex of telo15Z and NT similar to that of telo15 and NT was confirmed by the ion peak at *m/z* 1406.21 (Figure 1D). The fact that the guanine N7 is essential for the formation of a telo15 dimer, but not for the NT-bound complex, strongly suggested that NT binds to the Watson–Crick face of G and Z (Scheme 1B). Isothermal titration calorimetry[29] revealed that the binding constant of NT to telo15 was $5.71 \times 10^6\ M^{-1}$, with the titration curve fitting well to a 1:1 binding isotherm (see Figure S1 in the Supporting Information).

The structural changes of telo15 upon NT binding suggested by ESI-TOF MS measurements were supported by the absorbance changes at 260 and 295 nm (Figure 2). The melting of duplex to a single strand was monitored at 260 nm, whereas the melting of the quadruplex was monitored at 295 nm.[30] Since the G-quadruplex was stabilized by potassium cations, the measurements were carried out in 500 mM KCl. The absorption of telo15 at 295 nm decreased with increasing temperature to give a melting temperature of the G-quadruplex at 39.6 °C. In marked contrast, no apparent T_m of telo15Z was observed at 295 nm due to its inability to form a G-quadruplex (Figure 2A). Neither telo15 nor telo15Z showed apparent absorbance changes at 260 nm (data not shown). In the presence of NT, melting of NT-bound telo15 and telo15Z was clearly observed at 260 nm with T_m values of 62.8 and 71.3 °C, respectively (Figure 2B). The structural changes of telo15 and telo15Z were also clearly shown by CD spectra, with strong induced CD (Figure 3). The CD spectral change for telo15 while titrating with NT showed isodichroic points that indicated the single

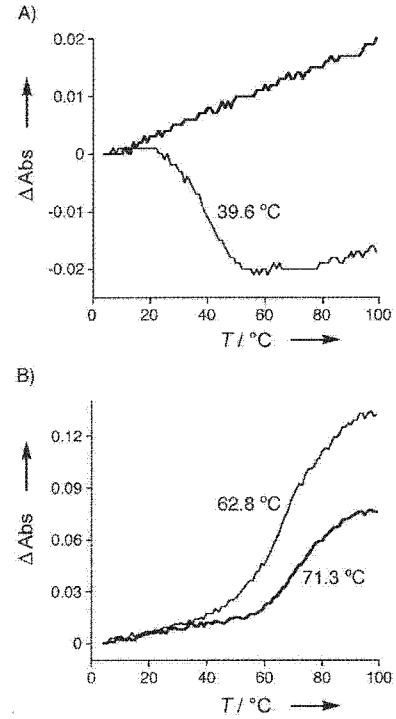

Figure 2. Thermal denaturation profiles of telo15 (thin line) and telo15Z (bold line; 5 μM) obtained in the absence and presence of NT (30 μM) in 500 mM KCl and 10 mM sodium cacodylate buffer (pH 7.0) from 4 to 98 °C with a heating rate of 1 °C min^{-1}. A) Absorbance changes at 295 nm in the absence of NT. B) Absorbance changes at 260 nm in the presence of NT. ΔAbs was obtained from the change in absorption of the solution before (4 °C) and after heating. The absorption change of NT was further subtracted from the data. The T_m calculated by the median method is shown in the figure.

transition between the two structural states. The isodichroic points were not clear for the structural change for telo15Z, because telo15Z does not have a particular struture in the absence of NT, as shown by the T_m measurements. The data from ESI-TOF MS, UV melting, and CD spectra indicated that 1) NT did not bind to the G-quadruplex form of telo15, 2) NT binding did not involve hydrogen bonds to G-N7, and 3) NT-bound structures had spectroscopic characteristics that resembled those of dsDNA; this suggested a hairpin formation of telo15 upon NT binding.

The possible hairpin form of telo15 involves a cluster of G–G mismatches in the stem region. To clarify the binding sites of NT among three G–G mismatches (GGa, GGb, and GGc), UV melting profiles of six mutant oligomers of telo15 were measured in the absence and presence of NT (Figure 4). The T_m of telo15 in 100 mM NaCl was too low to be detected, but was 71.2 °C in the presence of NT, that is, 8.4 °C higher than the T_m in 500 mM KCl. Mutant sequences telo15a and telo15b, in which GGa and GGb were replaced with an A–T base pair, did not show a measurable T_m, as for telo15. In the presence of NT, the T_m of telo15a was 75.0 °C, that is, 3.8 °C higher than that of telo15; this showed that substitution of GGa had negligible effects on NT binding. In marked contrast, the T_m of telo15b was 43.5 °C, that is, 27.7 °C lower than that of telo15. Likewise, the

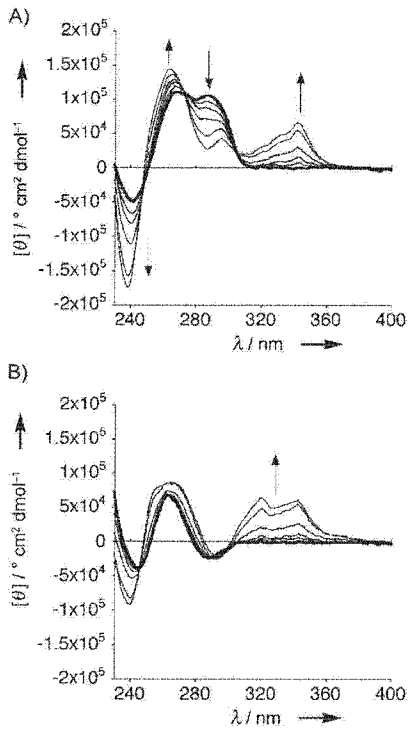

Figure 3. CD spectra of telo15 and telo15Z (5 μM) in the presence (thin line) and absence (bold line) of NT. The CD measurements were carried out with A) telo15 and B) telo15Z in 500 mM KCl and 10 mM sodium cacodylate buffer (pH 7.0) while titrating with NT (0, 0.5, 1, 2, 4, 6 μM) at 25 °C.

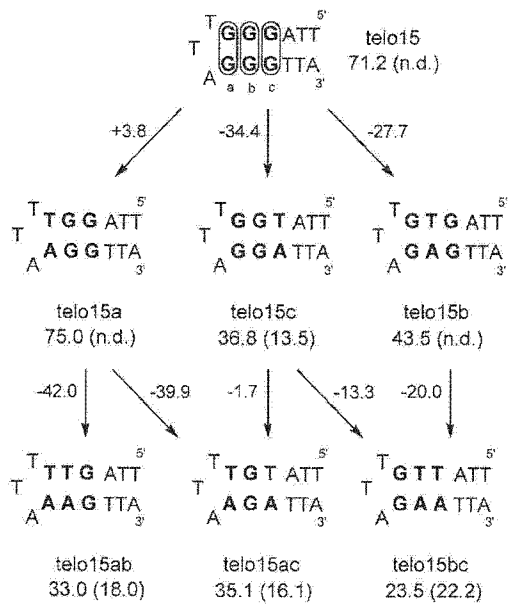

Figure 4. Possible hairpin structures of telo15 mutants (5 μM) and their T_m (°C) in the presence of NT (30 μM) in 100 mM NaCl and 10 mM sodium cacodylate (pH 7.0). UV melting profiles were measured at 260 nm. The T_m of the mutants is shown in parenthesis, n.d. = not detected. The numbers beside the arrows indicate the increase (+) or decrease (−) in T_m between the two mutants.

T_m of telo15c was 36.8 °C, a difference of 34.4 °C between telo15 and telo15c in the presence of NT. The subsequent substitution of GGb in telo15a to give telo15ab, and GGc in telo15a to give telo15ac, resulted in decreases of T_m by 42.0 and 39.9 °C, respectively. The substitution of GGc in telo15b and GGb in telo15c, both giving telo15bc, also decreased the T_m by 20.0 °C and 13.3 °C, respectively. Telo15bc was not stabilized by NT at all, as judged by the 1.3 °C increase in T_m in the presence of NT. The substitution of GGa in telo15b to give telo15ab led to a T_m decrease of 10.5 °C. Furthermore, the substitution of GGa in telo15c to give telo15ac had almost no effect. A large decrease in T_m when a cluster of GGb and GGc was modified indicated that both GGb and GGc were essential for the strong and simultaneous stabilization of, and hairpin formation in, telo15 by NT, whereas GGa was only very weakly effective on NT binding. The weak binding of NT to GGa was most likely because GGa was directly neighboring the TTA hairpin loop. Binding of NT to GGa would cause strain in the hairpin loop and was not energetically favorable.

The data described here suggested that NT induced a hairpin structure in telo15 with a 1:1 stoichiometry of binding. The novel mode of NT binding to the human telomere sequence described in these studies would be useful for the design of next-generation molecules that would show more potent binding to the sequence. Human telomere repeats form parallel and a mixed parallel/antiparallel conformers according to the presence of potassium and sodium cations, respectively.[11–15] Furthermore, the stability of the G-quadruplex structures is likely to depend on the repeat length. It is particularly informative to evaluate whether NT binds to long stretches of human telomere repeats under physiological conditions and can cause inhibition of the telomerase function. Finally, strong stabilization of two consecutive G–G mismatches by NT implies that NT might bind to other biologically important G-rich sequences, such as a promoter region[31] and a CGG trinucleotide repeat[32] by hairpin formation.

Experimental Section

Preparation of NT: A 25% glutaraldehyde solution saturated with NaCl was extracted with $CHCl_3$. The organic phase was evaporated to dryness to give glutaraldehyde as a viscous liquid. Glutaraldehyde (12 mg, 0.12 mmol) and $NaBH_3CN$ (18.7 mg, 0.30 mmol) were added to a solution of ND (110 mg, 0.25 mmol) in MeOH adjusted to pH 5 with acetic acid. The mixture was stirred at room temperature for 10 min, then poured into $CHCl_3$ and washed with brine. The organic layer was dried over Na_2SO_4 and evaporated in vacuo. The crude residue was purified by preparative thin-layer chromatography (TLC) to produce NT (34.5 mg, 15%) as a white solid. ^1H NMR (CD_3OD, 400 MHz) $\delta = 8.10$ (d, $J = 8.8$ Hz, 4H), 7.83 (d, $J = 8.4$ Hz, 4H), 7.83 (d, $J = 8.8$ Hz, 4H), 7.13 (d, $J = 8.4$ Hz, 4H), 2.79 (t, $J = 6.0$ Hz, 8H), 2.59 (s, 12H), 2.62–2.56 (8H), 2.53 (t, $J = 7.2$ Hz, 4H), 1.67 (m, 4H), 1.44 (m, 2H); ^{13}C NMR (CD_3OD, 100 MHz) $\delta = 174.1$, 163.7, 155.0, 154.9, 139.6, 138.2, 122.4, 119.4, 115.5, 55.2, 50.4, 35.5, 27.4, 26.5, 25.0; FABMS (NBA), *m/e* 955 $[M+H]^+$; HRMS calcd for $C_{53}H_{59}O_4N_{14}$: 955.4844 $[M+H]^+$; found: 955.4841.

General procedure for ESI-TOF MS analysis of the binding complex: DNA duplex solutions (20 μM) in 50% methanol containing

NH_4OAc (100 mM) were measured with various ligands in the negative mode of ESI-TOF MS (JEOL AccuTOF JMS-T100N). Nitrogen was used as the desolvation gas, as well as a nebulizer. Conditions for ESI-TOF MS were as follows: orifice 1 temperature and desolvation room temperature were not controlled, needle voltage −2100 V, ring-lens voltage −5 V, orifice 1 voltage −45 V, orifice 2 voltage −6 V.

Thermal denaturation profiles: UV melting experiments of **telo15** and its mutants were carried out with DNA oligomer (5 μM) in sodium cacodylate (10 mM, pH 7.0) containing NaCl (100 mM). The absorbance of the sample was monitored at 260 or 295 nm from 4 °C to 98 °C with a heating rate of 1 °C min^{-1} in the absence and presence of various concentrations of ligands. T_m values were calculated by using the median method. Measurement of the G-quadruplex of **telo15** was carried out in KCl (500 mM) instead of NaCl (100 mM). The change in absorbance was obtained from the following equation:

$$\Delta Abs = Abs_{temp} - Abs_{4\,^\circ C} - (NT\,Abs_{temp} - NT\,Abs_{4\,^\circ C})$$

Here Abs_{temp} is the absorption of **NT-telo15** at a specific temperature, and $NTAbs_{temp}$ is the absorption of **NT** at that temperature.

Keywords: inhibitors · ligand effects · mismatches · telomere repeats

[1] C. W. Greider, *Annu. Rev. Biochem.* **1996**, *65*, 337–365.
[2] E. H. Blackburn, *Nature* **1991**, *350*, 569–573.
[3] C. B. Harley, A. B. Futcher, C. W. Greider, *Nature* **1990**, *345*, 458–460.
[4] N. D. Hastie, M. Dempster, M. G. Dunlop, A. M. Thompson, D. K. Green, R. C. Allshire, *Nature* **1990**, *346*, 866–868.
[5] S. E. Holt, J. W. Shay, *J. Cell. Physiol.* **1999**, *180*, 10–18.
[6] J. L. Mergny, C. Hélène, *Nat. Med.* **1998**, *4*, 1366–1367.
[7] S. Neidle, G. Parkinson, *Nat. Rev. Drug Discovery* **2002**, *1*, 383–393.
[8] L. H. Hurley, *Nat. Rev. Cancer* **2002**, *2*, 188–200.
[9] S. M. Kerwin, *Curr. Pharm. Des.* **2000**, *6*, 441–478.
[10] S. Neidle, G. N. Parkinson, *Curr. Opin. Struct. Biol.* **2003**, *13*, 275–283.
[11] G. N. Parkinson, M. P. H. Lee, S. Neidle, *Nature* **2002**, *417*, 876–880.
[12] Y. Wang, D. J. Patel, *Structure* **1993**, *1*, 263–282.
[13] Y. Xu, Y. Noguchi, H. Sugiyama, *Bioorg. Med. Chem.* **2006**, *14*, 5584–5591.
[14] A. Ambrus, D. Chen, J. Dai, T. Bialis, R. A. Jones, D. Yang, *Nucleic Acids Res.* **2006**, *34*, 2723–2735.
[15] K. N. Luu, A. T. Phan, V. Kuryavyi, L. Lacroix, D. J. Patel, *J. Am. Chem. Soc.* **2006**, *128*, 9963–9970.
[16] J. F. Riou, L. Guittat, P. Mailliet, A. Laoui, E. Renou, O. Petitgenet, F. Megnin-Chanet, C. Hélène, J. L. Mergny, *Proc. Natl. Acad. Sci. USA* **2002**, *99*, 2672–2677.
[17] D. F. Shi, R. T. Wheelhouse, D. Sun, L. H. Hurley, *J. Med. Chem.* **2001**, *44*, 4509–4523.
[18] K. Shin-ya, K. Wierzba, K. Matsuo, T. Ohtani, Y. Yamada, K. Furihata, Y. Hayakawa, H. Seto, *J. Am. Chem. Soc.* **2001**, *123*, 1262–1263.
[19] W. Duan, A. Rangan, H. Vankayalapati, M. Y. Kim, Q. Zeng, D. Sun, H. Han, O. Y. Fedoroff, D. Nishioka, S. Y. Rha, E. Izbicka, D. D. Von Hoff, L. H. Hurley, *Mol. Cancer Ther.* **2001**, *1*, 103–120.
[20] S. M. Haider, G. N. Parkinson, S. Neidle, *J. Mol. Biol.* **2003**, *326*, 117–125.
[21] A. M. Burger, F. P. Dai, C. M. Schultes, A. P. Reszka, M. J. Moore, J. A. Double, S. Neidle, *Cancer Res.* **2005**, *65*, 1489–1496.
[22] R. A. Heald, C. Modi, J. C. Cookson, I. Hutchinson, C. A. Laughton, S. M. Gowan, L. R. Kelland, M. F. G. Stevens, *J. Med. Chem.* **2002**, *45*, 590–597.
[23] M. J. B. Moore, F. Cuenca, M. Searcey, S. Neidle, *Org. Biomol. Chem.* **2006**, *4*, 3479–3488.
[24] A. T. Phan, V. Kuryavyi, H. Y. Gaw, D. J. Patel, *Nat. Chem. Biol.* **2005**, *3*, 167–173.
[25] K. Nakatani, S. Sando, I. Saito, *Nat. Biotechnol.* **2001**, *19*, 51–55.
[26] K. Nakatani, S. Sando, H. Kumasawa, J. Kikuchi, I. Saito, *J. Am. Chem. Soc.* **2001**, *123*, 12650–12657.
[27] K. Nakatani, S. Hagihara, S. Sando, S. Sakamoto, K. Yamaguchi, C. Maesawa, I. Saito, *J. Am. Chem. Soc.* **2003**, *125*, 662–666.
[28] J. L. Beck, M. L. Colgrave, S. F. Ralph, M. M. Sheil, *Mass Spectrom. Rev.* **2001**, *20*, 61–87.
[29] A. N. Lane, T. C. Jenkins, *Q. Rev. Biophys.* **2000**, *33*, 255–306.
[30] J. L. Mergny, A. T. Phan, L. Lacroix, *FEBS Lett.* **1998**, *435*, 74–78.
[31] J. Seenisamy, E. M. Rezler, T. J. Powell, D. Tye, V. Gokhale, C. S. Joshi, A. Siddiqui-Jain, L. H. Hurley, *J. Am. Chem. Soc.* **2004**, *126*, 8702–8709.
[32] P. J. Hagerman, R. J. Hagerman, *Am. J. Hum. Genet.* **2004**, *74*, 805–816.

Received: December 22, 2006
Published online on ■■ ■■, 2007

The single-stranded region of the d-(TTAGGG) repeat is known to form a G-quadruplex structure in vitro. We report here a novel naphthyridine tetramer (NT) ligand that induces a nonquadruplex structure in the single-stranded region of the human telomeric sequence.

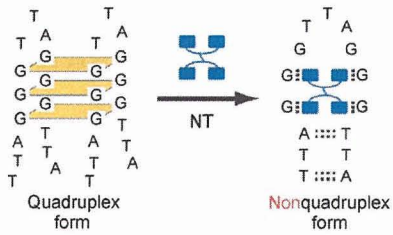

*Y. Goto, S. Hagihara, M. Hagihara, K. Nakatani**

■■–■■

Small-Molecule Binding to the Nonquadruplex Form of the Human Telomeric Sequence

Nucleic Acids Symposium Series No. 50 87–88
doi:10.1093/nass/nrl043

Control of DNA hybridization by photoswitchable mismatch binding ligands

Chikara Dohno, Shin-nosuke Uno and Kazuhiko Nakatani

The Institute of Scientific and Industrial Research, Osaka University, 8-1 Mihogaoka, Ibaraki 567-0047, Japan

ABSTRACT

We herein demonstrate that mismatch binding ligands (MBL) can function as a molecular glue which brings two single stranded DNA (ssDNA) together to form the double stranded DNA (dsDNA). Incorporation of a photoisomerizable azobenzene linkage provides further ability of reversibly controlling duplex stability with light.

INTRODUCTION

Sequence-specific hybridization property of DNA constitutes the indispensable basis for the essential functions of DNA. For regulation of biological functions and construction of DNA-based materials, controlling DNA hybridization by external stimuli has become an increasingly important. Studies toward controlling or modulating the DNA hybridization with chemically modified oligonucleotides have been reported previously.[1-5] We here describe an approach to turn on the duplex formation by a small synthetic ligand from two natural non-modified ssDNA. In addition, reversible photo-control of the duplex stability has been explored by the introduction of photo-isomerizable moiety into MBL.

RESULTS AND DISCUSSION

In switching the state of DNA hybridization, large stability difference between ssDNA-MBL and dsDNA-MBL complex provides an ideal switching threshold. Recent studies on the binding of MBL to the trinucleotide repeats revealed a novel mode of ligand binding to the mismatched DNA duplex, and this finding motivated us to develop a molecular glue of DNA.[6-8] The naphthyridine carbamate dimer (**NC**) selectively binds to the 5'-CGG-3'/5'-CGG-3' sequence (CGG/CGG) involving a G-G mismatch flanked by two C-G base pairs with a stoichiometry of **NC**:DNA to be 2:1 (Figure 1).[7] The **NC** binding to the CGG/CGG sequence induced two cytosines to be out of the π-stack. Since the unpaired cytosines are not directly engaged in the formation of **NC**-DNA complex, we anticipated that the flipped out cytosine could be substituted with other nucleotide base, such as thymine. The 5'-TGG-3'/5'-TGG-3' (TGG/TGG) sequence consists of three contiguous T-G, G-G, and G-T mismatches, and therefore, the dsDNA formation is energetically unfavourable. These ssDNA, which do not spontaneously hybridize with each other, could be adhered by the **NC**-binding to the TGG/TGG sequence.[8] In fact, 11-mer 5'-(CCTT TGG TCAG)-3'/5'-(CTGA TGG AAGG)-3' were present as a ssDNA at room temperature due to the three contiguous mismatches. In marked contrast, melting temperature (T_m) of the 58.8 °C was observed in the presence of 100 μM **NC**, suggesting the formation of **NC**-bound TGG/TGG duplex.

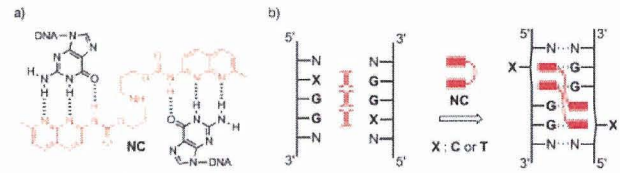

Fig. 1 (a) Complementary hydrogen bonding between **NC** and two guanine bases. (b) A schematic illustration of the **NC** binding to the XGG/XGG sequence. **NC** induces the DNA hybridization.

MBL can act as a molecular glue which brings two ssDNA together to form the dsDNA. However, MBL does not have an ability to unfold the once formed dsDNA, and thus the induction of dsDNA formation by the MBL binding is fundamentally unidirectional. In order to control the DNA hybridization reversibly, we functionalized the MBL to be a photo-responsive DNA binder. **NC** is constituted of a base recognizing naphthyridine moiety and a flexible linker connecting the two naphthyridines. The linker is replaced by a photochromic azobenzene moiety for the design of a photo-switchable MBL, **NC_2Az** (Fig. 2). Azobenzene undergoes a reversible photoisomerization, which changes the relative orientations and positions of the naphthyridine units in **NC_2Az**, and thus modulates the binding ability.

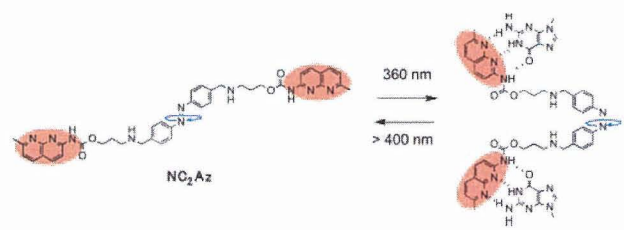

Fig. 2 Photoisomerization of **NC_2Az**. UV light induces *trans* to *cis* isomerization of azobenzene moiety of **NC_2Az**, whereas visible light results in *cis* to *trans* isomerization.

Before photoirradiation, **NC_2Az** exists in the pure *trans*-form. Photoirradiation at a wavelength of 360 nm led to the *trans* to *cis* isomerization of **NC_2Az**. The *cis*/*trans* ratio after the irradiation was determined by HPLC detected at the isosbestic point. The photostationary state reached after 5 min irradiation consisted of a nearly equimolar mixture of *cis*- and *trans*-**NC_2Az**. The equilibrium mixtures reverted to the pure *trans* form of **NC_2Az** upon irradiation of visible light at 430 nm.

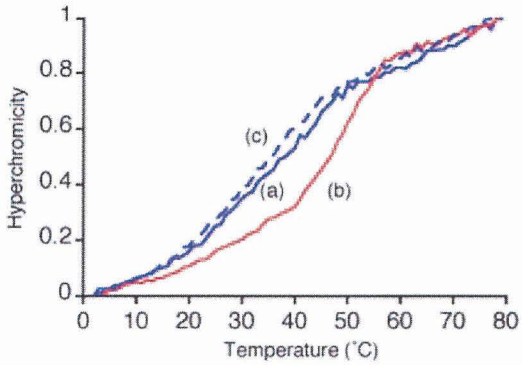

Fig. 3 Thermal melting curves of GG-mismatch containing DNA duplex (4.5 μM) in the presence of **NC_2Az** (18.2 μM). The absorbance at 260 nm was measured in 10 mM Na·cacodylate buffer (pH 7.0) containing 0.1 M NaCl. Temperature was increased from 2 to 80 °C at a rate of 1°C/min. T_m was calculated with the median method. (a) Without photoirradiation. (b) After photoirradiation at 360 nm for 5min. (c) (b) followed by irradiation at 430 nm for 5 min.

The **NC_2Az** binding to the mismatched DNA was evaluated by measuring T_m of the **NC_2Az**-DNA complex. T_m measurements were carried out using 11-mer DNA duplex 5'-(CTAA CGG AATG)-3'/5'-(CATT CGG TTAG)-3' containing a CGG/CGG mismatch sequence in the presence of **NC_2Az**. Without photoirradiation, **NC_2Az** exists in the *trans*-form, and the T_m of 32.7°C was obtained (Figure 3a). Exposure of **NC_2Az** to 360 nm light increased the T_m value by 15.2 °C (T_m = 48.0°C, Figure 3b). Interestingly, the percentage of *cis*-**NC_2Az** (75%) was higher than that in the absence of the mismatched DNA. These results indicate *cis*-form of **NC_2Az** has higher binding ability to the CGG/CGG sequence. This is most likely because the nonplanar *cis*-azobenzne linkage in **NC_2Az** allows two naphthyridine units to be placed in the appropriate position for binding (Fig. 4). Thus, *trans* to *cis* photoisomerization of **NC_2Az** facilitated the formation of GG-mismatch-containing DNA duplex. Importantly, this duplex stabilization by **NC_2Az** was fully reversible. Irradiation of 430 nm light induced *cis* to *trans* transformation, and destabilized the duplex back to the normal mismatch-containing DNA (Fig. 3c).

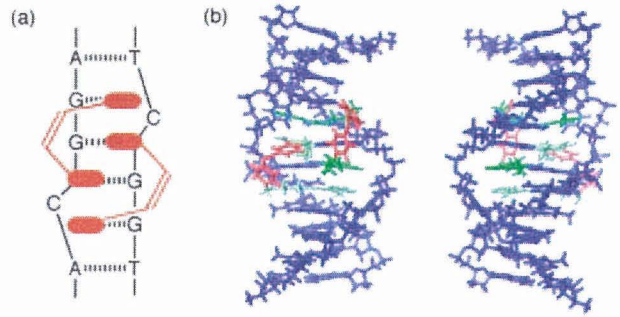

Fig. 4 (a) Schematic representation of the binding of *cis*-**NC_2Az** to CGG/CGG sequence. (b) Molecular modelling of the *cis*-**NC_2Az**-CGG/CGG complex. The model structure was optimized by use of the AMBER* force field in water with MacroModel Version 9.1.

CONCLUSION

MBL, such as **NC**, promotes DNA hybridization between the mismatch-containing DNAs by the formation of stable MBL-DNA complex. The introduction of a photochromic azobenzene linkage into MBL permits reversible control of duplex stability of the mismatch-containing DNA. The molecules described here represent a new class of compounds that function as a molecular glue not only in DNA hybridization but also in modulating the DNA secondary structures.

REFERENCES

1. Asanuma, H., Ito, T., Yoshida, T., Liang, X., Komiyama, M. (1999) *Angew. Chem. Int. Ed.*, **38**, 2393-2395.
2. Asanuma, H., Liang, X., Yoshida, T., Yamazawa, A., Komiyama, M. (2000) *Angew. Chem. Int. Ed.*, **39**, 1316-1318.
3. Liu, Y., Sen, D. (2004) *J. Mol. Biol.*, **341**, 887-892
4. Ghosn, B., Haselton, F. R., Gee, K. R., Monroe, W. T. (2005) *Photochem. Photobiol.*, **81**, 953-959.
5. Hamad-Schifferli, K., Schwartz, J. J., Santos, A. T., Zhang, S. G., Jacobson, J. M. (2002) *Nature*, **415**, 152-155.
6. Nakatani, K., Hagihara, S., Goto, Y., Kobori. A., Hagihara, M., Hayashi, G., Kyo, M., Nomura, M., Mishima, M., Kojima, C. (2005) *Nat. Chem. Biol.*, **1**, 39-43.
7. Peng, T., Nakatani, K. (2005) *Angew. Chem. Int. Ed.*, **44**, 7280-7283.
8. Peng, T., Dohno, C., Nakatani, K. *Angew. Chem. Int. Ed.*, in press.

Nucleic Acids Symposium Series No. 50 147–148
doi:10.1093/nass/nrl073

Inhibition of DNA replication by a d(CAG) repeat binding ligand

Masaki Hagihara and Kazuhiko Nakatani

The Institute of Scientific and Industrial Research, Osaka University, Mihogaoka 8-1, Ibaraki, Osaka 567-0047, Japan

ABSTRACT

Trinucleotide repeat expansions in genomic DNA are the molecular basis of a number of genetic diseases. The $(CAG)_n$, $(CTG)_n$, and $(CGG)_n$ repeats share the common sequence CXG, and inherently produce a hairpin structure involving X–X mismatch base pairs flanked by two G–C base pairs. The chance of a strand slippage leading to the repeat expansion is considered to increase with increasing stability of the hairpin form. Here we show our synthetic ligand naphthyridine–azaquinolone (NA) stabilized a hairpin form of the $(CAG)_n$ repeat and inhibited the polymerase-mediated DNA synthesis.

INTRODUCTION

The expansion of (CAG)n trinucleotide repeats in genomic DNA is related to the pathogenesis of Huntington's disease. The CAG repeat range is normally 9–35, whereas 38 or more repeats are found in the diseased state[1,2,3]. Although the mechanism of repeat expansion remains unclear, it is believed to involve strand slippage during DNA synthesis mediated by the formation of an alternative hairpin structure. The hairpin form of (CAG)n repeats involves the intramolecular pairing of CAG/CAG triads, the central A–A mismatch base pairs being flanked by two G–C base pairs. Thus ligands that bind to the CAG/CAG triad also are expected to bind to the hairpin form of the (CAG)n repeats. We have previously reported that a naphthyridine–azaquinolone (**NA**) ligand binds with high affinity to the CAG/CAG triad and we have recently shown the solution structure of **NA**–CAG/CAG complex by NMR spectroscopy[4]. NMR analysis revealed that two **NA** molecules intercalate into DNA helix, with the 2-amino-1,8-naphthyridine moiety presenting complementary hydrogen bonding to guanine, and 8-azaquinolone moiety presenting fully complementary hydrogen bonding to adenine. Furthermore binding of two **NA** molecules causes extrusion of two cytosines to the outside of the DNA helix (Figure 1).

In order to evaluate whether **NA** induced hairpin structure in CAG repeats can show the biological roles in DNA replication processes, we performed the thermal stability of **NA**-induced hairpin structure with different (CAG)n repeat length. The polymerase stop assay clearly showed that the hairpin formation by **NA**-binding to the (CAG)n repeat sequence in the template inhibited DNA polymerase to synthesize DNA strands.

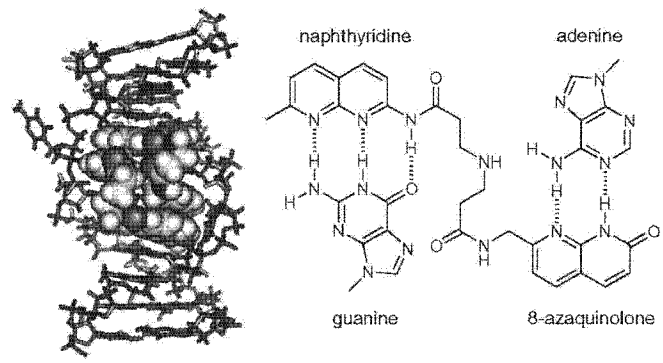

Figure 1 (a) Structure of **NA**–CAG/CAG complex. (b) The naphthyridine chromophore makes a complemental hydrogen bonding surface to guanine, whereas 8-azaquinolone is complementally to adenine.

RESULTS AND DISCUSSION

Strong **NA** binding to the CAG/CAG triad induced the formation of the **NA**-bound hairpin form in (CAG)n repeats DNA. The stabilization of hairpin structure was assessed by UV thermal denaturation studies. The thermal stability of $(CAG)_{10}$, ten repeats of CAG trinucleotides, was strongly enhanced by 24.7 °C in the presence of 20 μM **NA**.

Polymerase stop assay[5] was performed on the template containing ten repeat units of CAG sequence to test whether the hairpin structure induced by **NA** binding can interfere with the elongation of the (CAG)n repeat sequence. In the absence of **NA**, the 20-mer primer 5'-d(TAATACGACTCACTATAGGG)-3' that hybridized to the 3' end of the (CAG)n containing template was fully elongated by Klenow polymerase. As increasing the **NA** concentration, the intensity of the posed bands increased with a concomitant decrease of the fully elongated products. At 20 μM of **NA**, DNA synthesis by Klenow polymerase was almost stopped at the first CAG site (Figure 2). These results are consistent with a notion that inhibition of DNA polymerase was attributed to induced hairpin structure in CAG repeat DNA, but not to inhibition of Klenow DNA polymerase itself. These results showed that there was a good correlation between the thermal stability of induced hairpin structure and the inhibitory effects of DNA synthesis.

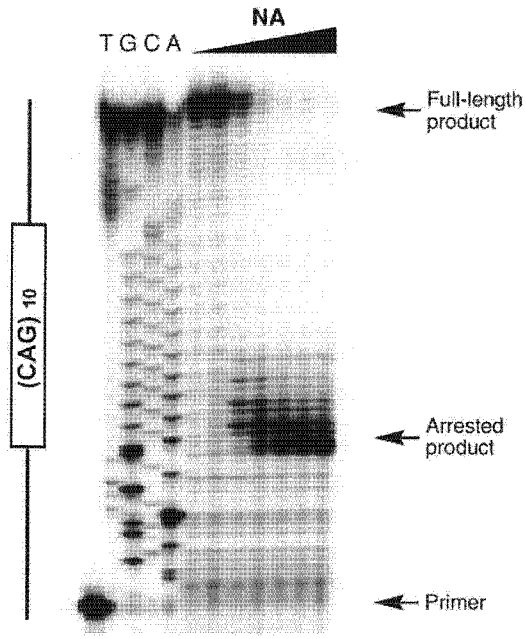

Figure 2 Concentration-dependent inhibition of Klenow DNA polymerase-mediated DNA synthesis with **NA** (0, 5, 10, 15, 20, 25, 30 μM) on a DNA template containing the $(CAG)_{10}$ sequence. The lane markers T, G, C, and A indicate the bases on the template strand. Arrows indicate the positions of full-length DNA synthesis product, the arrested product, and the free primer.

CONCLUSION

In conclusion, we found that **NA** leads to enhanced arrest of DNA synthesis by stabilizing an intrastrand hairpin structure formed by the (CAG)n repeat sequences. **NA** would be an important molecular probe for the repeat expansion mechanism and also effective therapeutic agents for genetic diseases.

REFERENCES

1. Wells, R. D., Warren, S. T. (1998) *Genetic Instabilities and Hereditary Neurological Disease. Academic Press, San Diego.*
2. Stine, O. C., Pleasant, N., Franz, M. L., Abbott, M. H., Folstein, S. E., Ross, C. A. (1993) *Hum. Mol. Genet.*, **2**, 1547-1549.
3. Ashley, C. T., Warren, S. T. (1995) *Annu. Rev. Genet.*, **29**, 703-728.
4. Nakatai, K., Hagihara, S., Goto. Y., Kobori, A., Hagihara, M., Hayashi, G., Kyo, M., Nomura, M., Mishima, M., Kojima, C. (2005) *Nature Chemical Biology*, **1**, 39-43.
5. Han, H., Hurley, L. H., Salazar, M. (1999) *Nucleic Acids Res.*, **27**, 537-542.

Nucleosides, Nucleotides, and Nucleic Acids, 25:613–624, 2006

ISSN: 1525-7770 print / 1532-2335 online
DOI: 10.1080/15257770600686454

Taylor & Francis
Taylor & Francis Group

NMR SPECTROSCOPIC STUDY OF A DNA DUPLEX WITH MERCURY-MEDIATED T-T BASE PAIRS

Yoshiyuki Tanaka, Hiroshi Yamaguchi, Shuji Oda, and Yoshinori Kondo
Graduate School of Pharmaceutical Sciences, Tohoku University, Aobayama, Aoba-ku, Sendai, Miyagi, Japan

Makoto Nomura and Chojiro Kojima *Graduate School of Biological Sciences, Nara Institute of Science and Technology, Ikoma, Nara, Japan*

Akira Ono *Department of Material and Life Chemistry, Faculty of Engineering, Kanagawa University, Kanagawa-ku, Yokohama, Kanagawa, Japan*

*Recently, we reported that T-T mismatches can specifically recognize Hg^{II} (T-Hg^{II}-T pair formation). In order to understand the properties of the T-Hg^{II}-T pair, we recorded NMR spectra for a DNA duplex, d(CCGG**TT**GTCC)•d(GGAC**TT**CGGG), with two successive T-T mismatches (Hg^{II}-binding sites). We assigned ^1H resonances for mercury-free and di-mercurated duplexes, and performed titration experiments with Hg^{II} by using 1D ^1H NMR spectra. Because of the above mentioned assignments, we could confirm the existence of mono-mercurated species, because individual components gave independent NMR signals in the titration spectra.*

Keywords ^1H NMR; Hg^{II}-mediated T-T base pair; Titration; Equilibrium

INTRODUCTION

It has been recently demonstrated that metal-mediated base pairs can be formed by replacing natural nucleobases with artificial metal chelators.[1–11] In addition, we demonstrated that a natural nucleobase, thymine, is also able to form a mercury-mediated T-T pair (T-Hg^{II}-T pair formation), and because of this property, DNA duplexes with T-Hg^{II}-T pairs could be used

Received 18 January 2006; accepted 14 February 2006.
This article is dedicated to Professor Eiko Ohtsuka on the occasion of her 70th birthday.
This work was supported by a grant-in-aid for Scientific Research (C) (18550114-06) from the Ministry of Education, Culture, Sports, Science and Technology, Japan. AO was supported by a grant-in-aid for Scientific Research (B) (16350090), and by The Mitsubishi Foundation.
Address correspondence to Yoshiyuki Tanaka, Ph.D., Laboratory of Molecular Transformation, Graduate School of Pharmaceutical Sciences, Tohoku University, Aobayama, Aoba-ku, Sendai, Miyagi 980-8578, Japan. E-mail: tanaka@mail.pharm.tohoku.ac.jp